Filtragem na Frequência e Transformada de Fourier

Prof. Vinícius de Oliveira

Brasília, 28 de Novembro de 2019

Transformada de Fourier Contínua 1-D

$$F\{f(t)\} = F(\mu) = \int_{-\infty}^{\infty} f(t)e^{-j2\pi\mu t}dt$$

$$f(t) = \int_{-\infty}^{\infty} F(\mu)e^{j2\pi\mu t}d\mu$$

Transformada de Fourier Contínua 1-D

$$f(t) = \begin{cases} 0 & \text{se } |t| > W/2 \\ A & \text{se } |t| \leq W/2 \end{cases}$$

$$\begin{aligned} F(\mu) &= \int_{-\infty}^{\infty} f(t) e^{-j2\pi\mu t} dt = \int_{-W/2}^{W/2} A e^{-j2\pi\mu t} dt \\ &= \frac{-A}{j2\pi\mu} \left[e^{-j2\pi\mu t} \right]_{W/2}^{W/2} = \frac{-A}{j2\pi\mu} \left[e^{-j\pi\mu W} - e^{j\pi\mu W} \right] \\ &= AW \frac{\sin(\pi\mu W)}{\pi\mu W} = AW \mathrm{sinc}(\mu W) \end{aligned}$$

Transformada de Fourier Contínua 1-D

$$f(t) = \begin{cases} 0 & \text{se } |t| > W/2 \\ A & \text{se } |t| \leq W/2 \end{cases}$$

$$F(\mu) = AW\,\text{sinc}(\mu W)$$

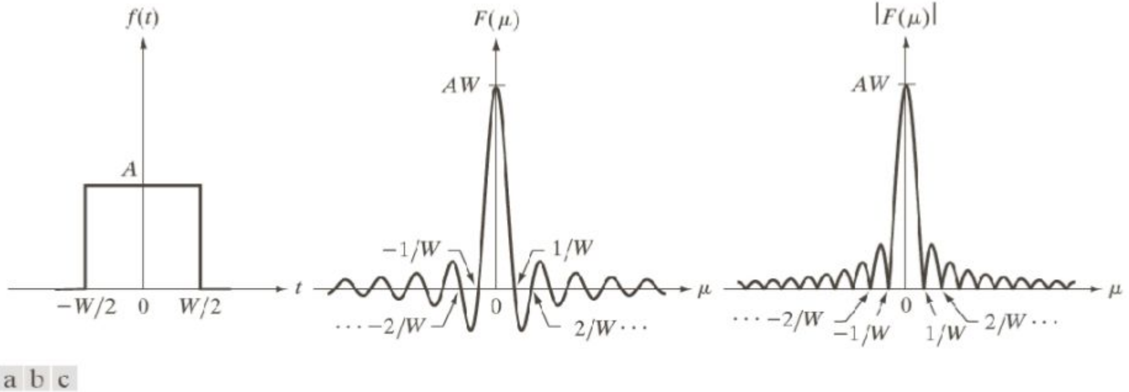

FIGURE 4.4 (a) A simple function; (b) its Fourier transform; and (c) the spectrum. All functions extend to infinity in both directions.

TF do Trem de impulsos

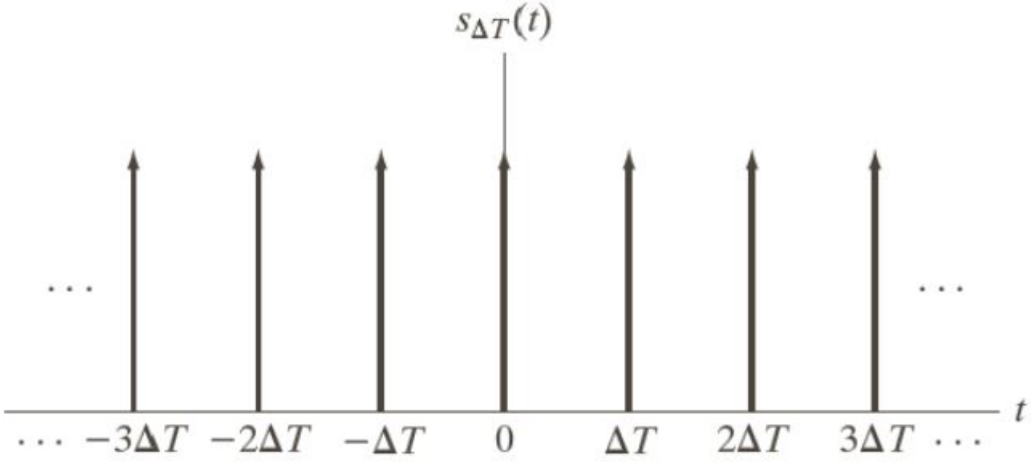

$$s_{\Delta T}(t) = \sum_{n=-\infty}^{\infty} \delta(t - n\Delta T)$$

Amostragem:

Sinal amostrado:

$$\tilde{f}(t) = f(t) \cdot s_{\Delta T}(t) = \sum_{n=-\infty}^{\infty} f(t)\delta(t - n\Delta T)$$

$$f_k = \int_{-\infty}^{\infty} f(t)\delta(t - n\Delta T)dt = f(k\Delta T)$$

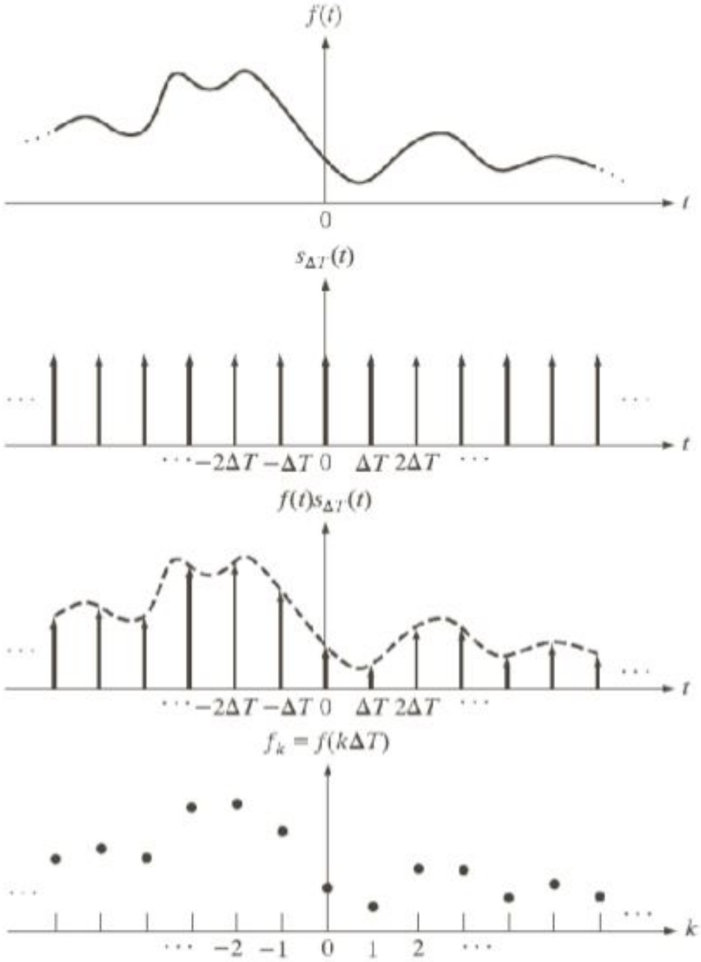

Amostragem:

$$\tilde{F}(\mu) = F\left\{\tilde{f}(t)\right\} = \tilde{F}(\mu) = F\left\{f(t) \cdot s_{\Delta T}(t)\right\}$$
$$= F(\mu) * F\left\{s_{\Delta T}(t)\right\} = F(\mu) * S(\mu)$$

$$S(\mu) = \frac{1}{\Delta T} \sum_{n=-\infty}^{\infty} \delta\left(\mu - \frac{n}{\Delta T}\right)$$

$$\tilde{F}(\mu) = F(\mu) * S(\mu) = \int_{-\infty}^{\infty} F(\tau) S(\mu - \tau) d\tau$$
$$= \frac{1}{\Delta T} \int_{-\infty}^{\infty} F(\tau) \sum_{n=-\infty}^{\infty} \delta\left(\mu - \tau - \frac{n}{\Delta T}\right) d\tau$$

Amostragem:

A TF do sinal amostrado:

- É uma sequência periódica e infinita de cópias de F(μ) deslocadas;
- Separação entre cópias de 1/ΔT;
- É uma função contínua(F(μ) é contínua);

$$\tilde{F}(\mu) = F(\mu) * S(\mu) = \int_{-\infty}^{\infty} F(\tau) S(\mu - \tau) d\tau$$

$$= \frac{1}{\Delta T} \int_{-\infty}^{\infty} F(\tau) \sum_{n=-\infty}^{\infty} \delta\left(\mu - \tau - \frac{n}{\Delta T}\right) d\tau$$

$$= \frac{1}{\Delta T} \sum_{n=-\infty}^{\infty} \int_{-\infty}^{\infty} F(\tau) \delta\left(\mu - \tau - \frac{n}{\Delta T}\right) d\tau$$

$$= \frac{1}{\Delta T} \sum_{n=-\infty}^{\infty} F\left(\mu - \frac{n}{\Delta T}\right)$$

Amostragem:

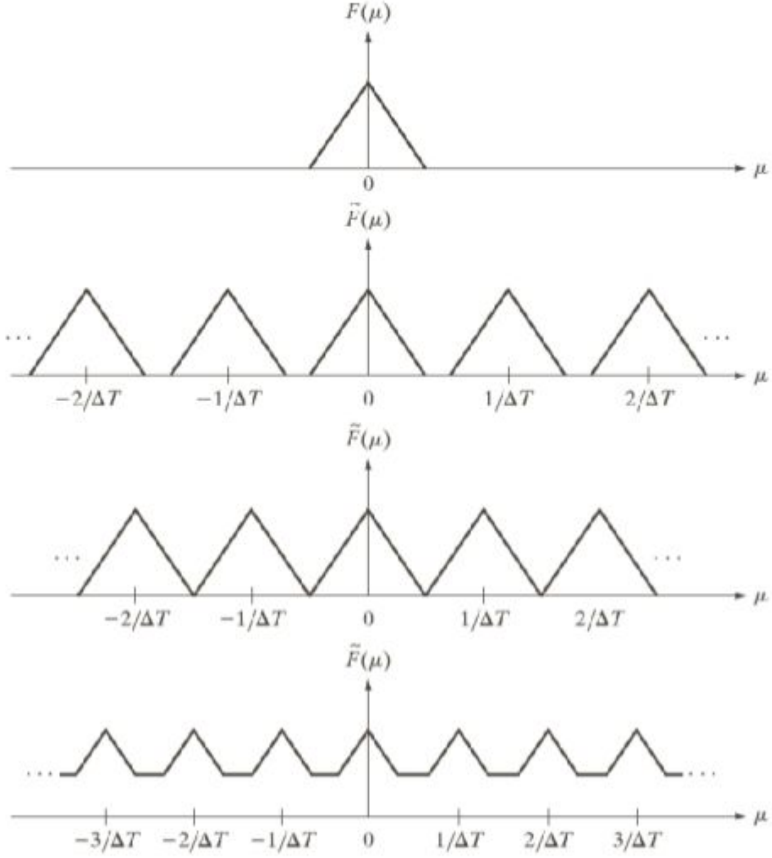

$$\frac{1}{\Delta T} > 2\mu_{max} = f_s$$

Taxa de Nyquist – Teorema de Amostragem

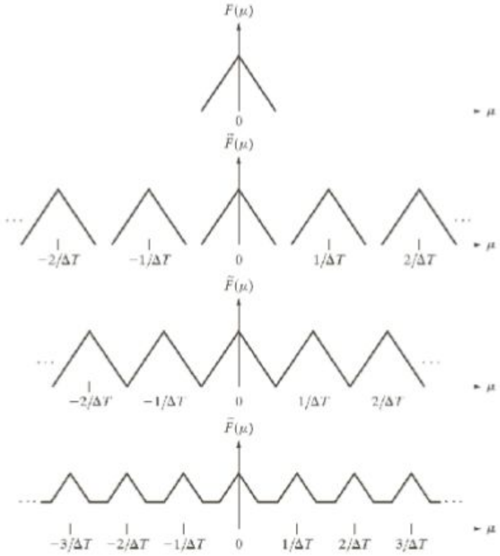

Sinais 2D

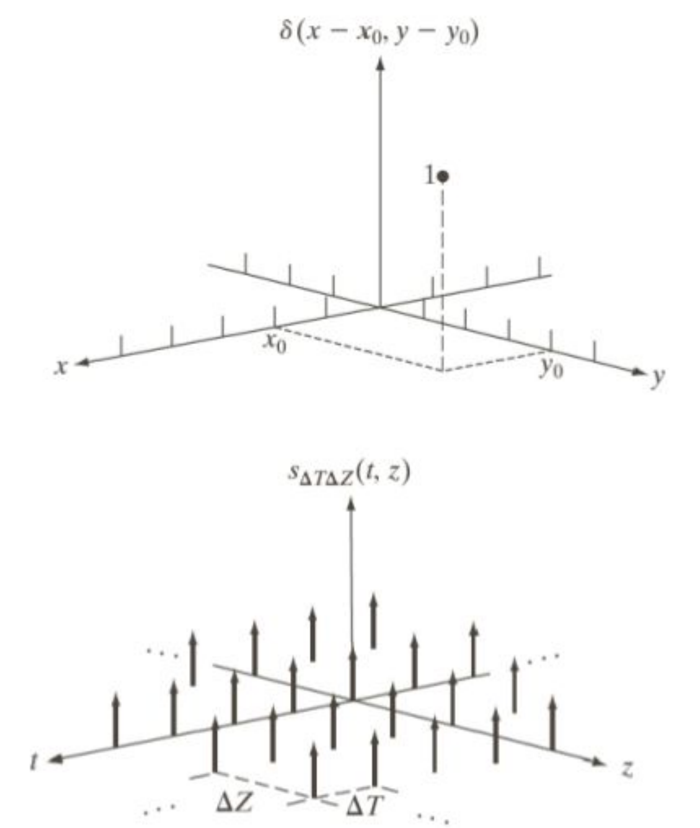

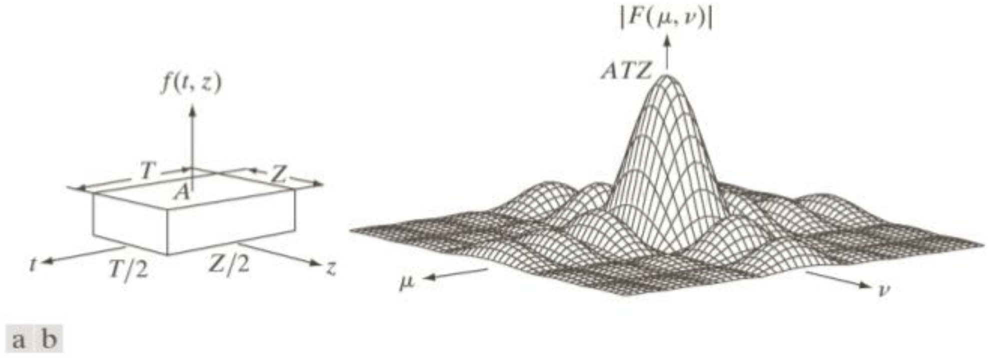

FIGURE 4.13 (a) A 2-D function, and (b) a section of its spectrum (not to scale). The block is longer along the t-axis, so the spectrum is more "contracted" along the μ-axis. Compare with Fig. 4.4.

Sinais 2D

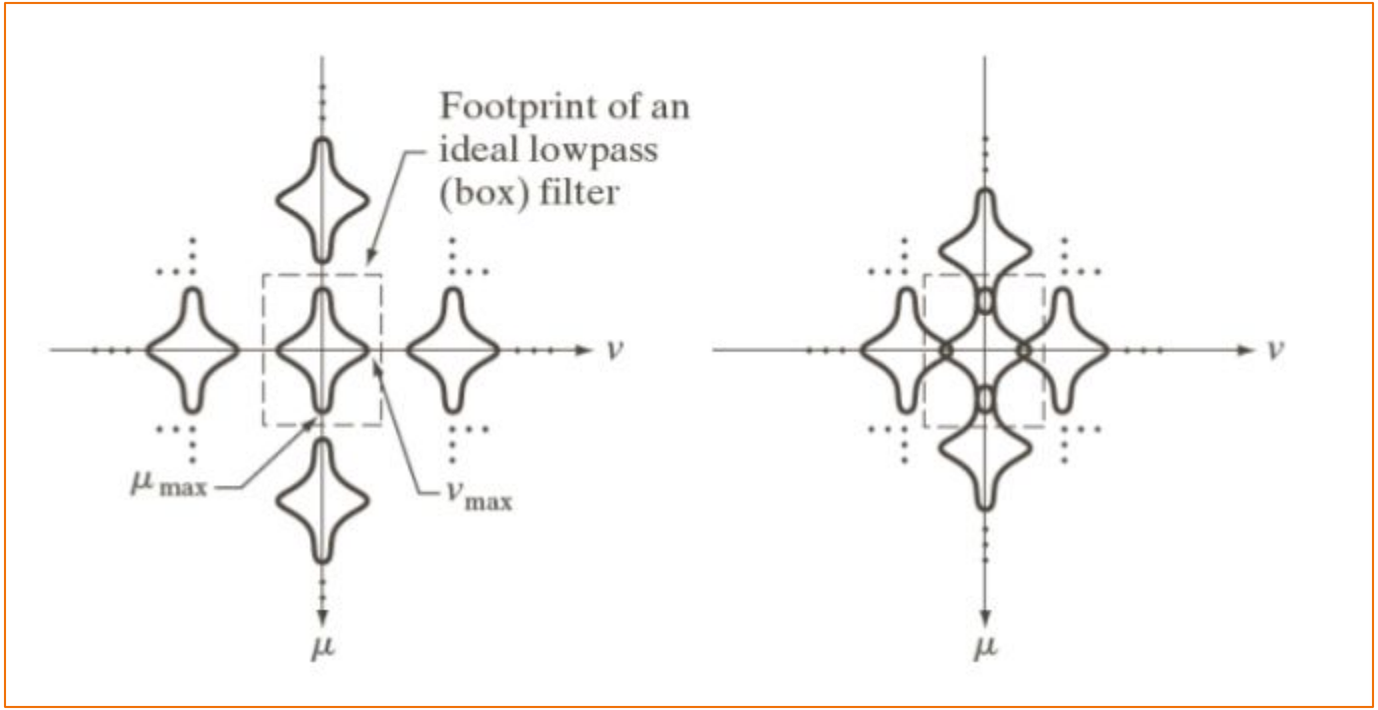

Aliasing 2D

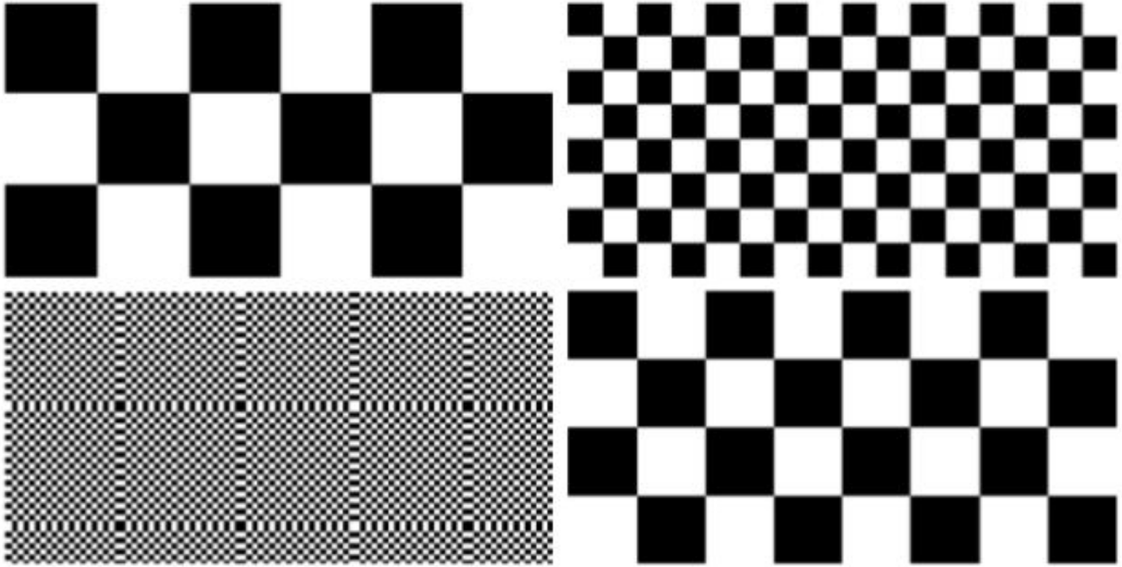

a b
c d

FIGURE 4.16 Aliasing in images. In (a) and (b), the lengths of the sides of the squares are 16 and 6 pixels, respectively, and aliasing is visually negligible. In (c) and (d), the sides of the squares are 0.9174 and 0.4798 pixels, respectively, and the results show significant aliasing. Note that (d) masquerades as a "normal" image.

Aliasing 2D

a b c

FIGURE 4.17 Illustration of aliasing on resampled images. (a) A digital image with negligible visual aliasing. (b) Result of resizing the image to 50% of its original size by pixel deletion. Aliasing is clearly visible. (c) Result of blurring the image in (a) with a 3×3 averaging filter prior to resizing. The image is slightly more blurred than (b), but aliasing is not longer objectionable. (Original image courtesy of the Signal Compression Laboratory, University of California, Santa Barbara.)

Aliasing 2D

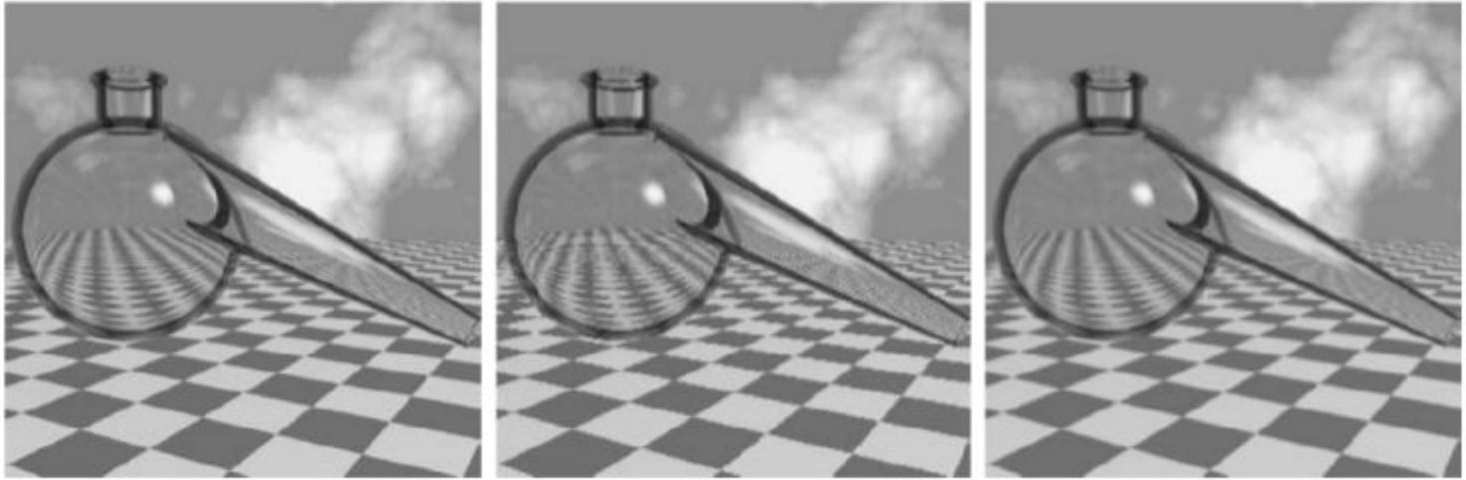

a b c

FIGURE 4.18 Illustration of jaggies. (a) A 1024 × 1024 digital image of a computer-generated scene with negligible visible aliasing. (b) Result of reducing (a) to 25% of its original size using bilinear interpolation. (c) Result of blurring the image in (a) with a 5 × 5 averaging filter prior to resizing it to 25% using bilinear interpolation. (Original image courtesy of D. P. Mitchell, Mental Landscape, LLC.)

Aliasing 2D

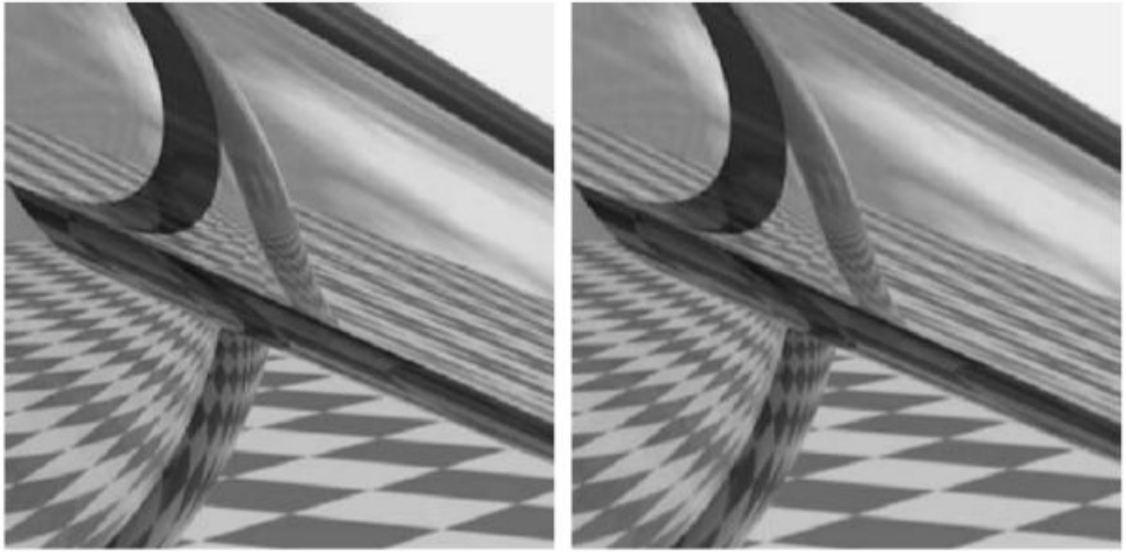

a b

FIGURE 4.19 Image zooming. (a) A 1024×1024 digital image generated by pixel replication from a 256×256 image extracted from the middle of Fig. 4.18(a). (b) Image generated using bi-linear interpolation, showing a significant reduction in jaggies.

Frequência no domínio do espaço de Imagens

A transformada de Fourier codifica:

- a freqüência espacial;
- a magnitude (positiva ou negativa);
- o ângulo de fase.

Obs: Um deslocamento do sinal no domínio do espaço não afeta a magnitude, entretanto, adiciona uma componente linear à fase.

Propriedades da TFD - 2D

Name	DFT Pairs
1) Symmetry properties	See Table 4.1
2) Linearity	$af_1(x, y) + bf_2(x, y) \Leftrightarrow aF_1(u, v) + bF_2(u, v)$
3) Translation (general)	$f(x, y)e^{j2\pi(u_0x/M + v_0y/N)} \Leftrightarrow F(u - u_0, v - v_0)$ $f(x - x_0, y - y_0) \Leftrightarrow F(u, v)e^{-j2\pi(ux_0/M + vy_0/N)}$
4) Translation to center of the frequency rectangle, $(M/2, N/2)$	$f(x, y)(-1)^{x+y} \Leftrightarrow F(u - M/2, v - N/2)$ $f(x - M/2, y - N/2) \Leftrightarrow F(u, v)(-1)^{u+v}$
5) Rotation	$f(r, \theta + \theta_0) \Leftrightarrow F(\omega, \varphi + \theta_0)$ $x = r\cos\theta \quad y = r\sin\theta \quad u = \omega\cos\varphi \quad v = \omega\sin\varphi$
6) Convolution theorem[†]	$f(x, y) \star h(x, y) \Leftrightarrow F(u, v)H(u, v)$ $f(x, y)h(x, y) \Leftrightarrow F(u, v) \star H(u, v)$

Propriedades da TFD - 2D

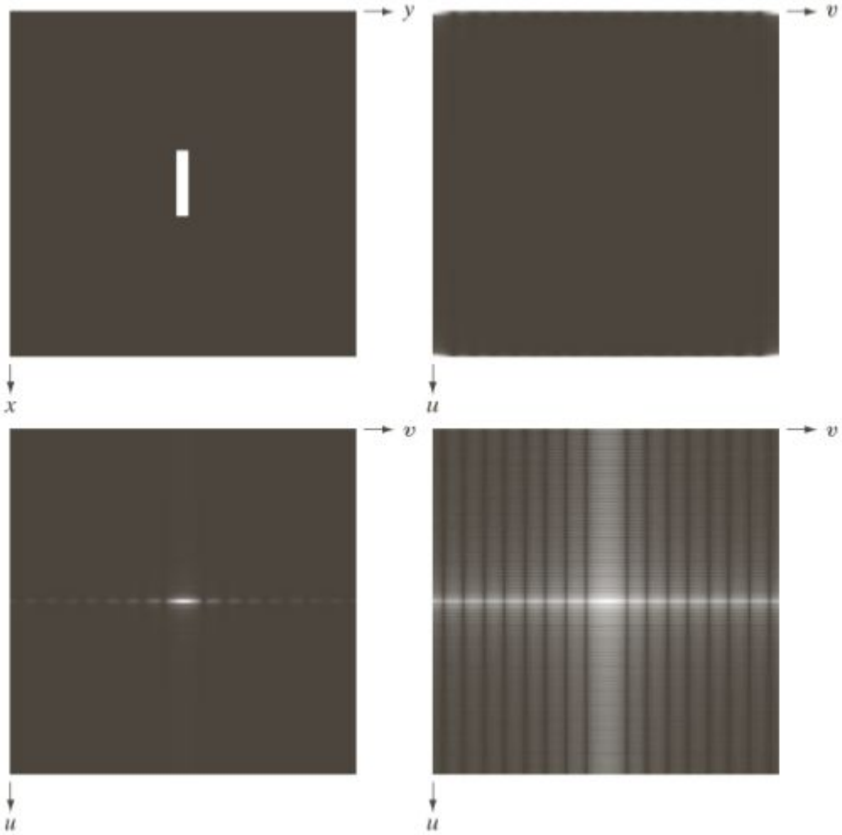

Propriedades da TFD - 2D

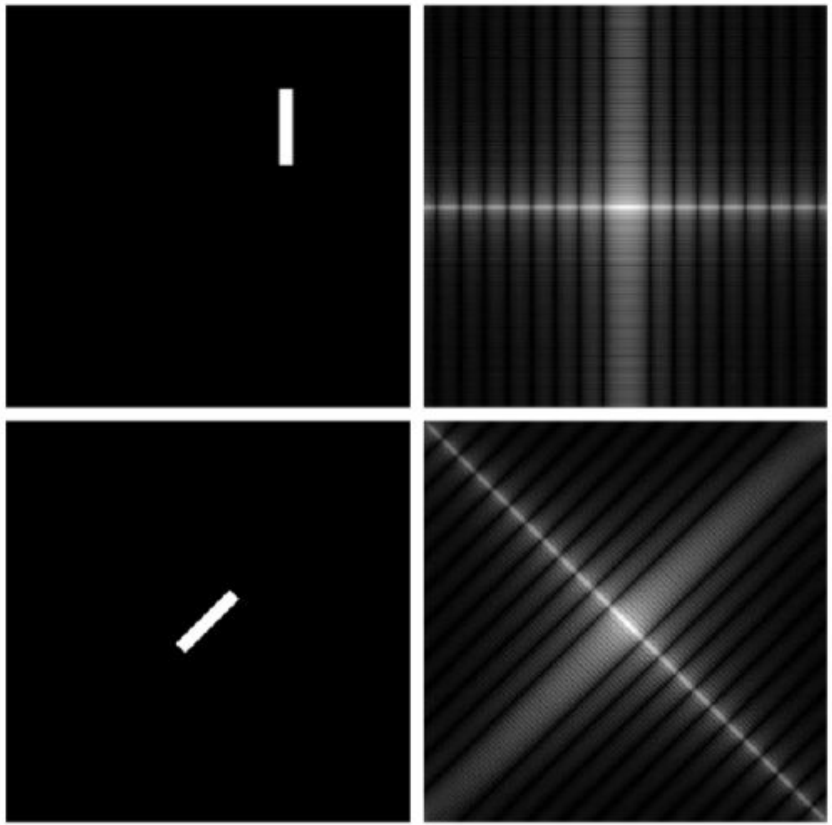

Propriedades da TFD - 2D

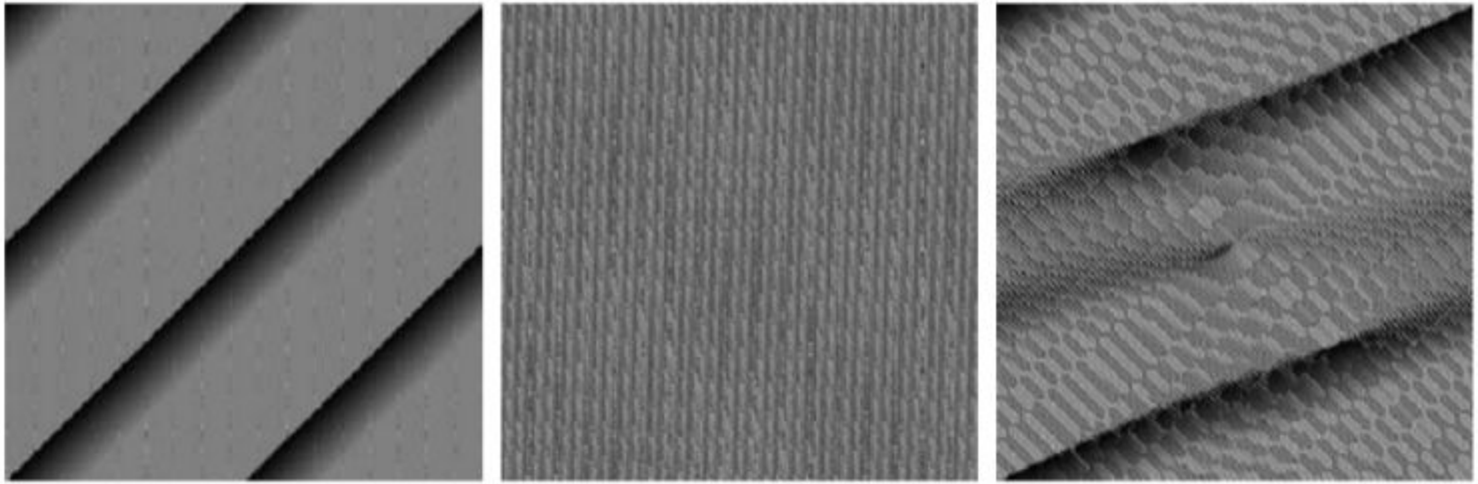

a b c

FIGURE 4.26 Phase angle array corresponding (a) to the image of the centered rectangle in Fig. 4.24(a), (b) to the translated image in Fig. 4.25(a), and (c) to the rotated image in Fig. 4.25(c).

Propriedades da TFD - 2D

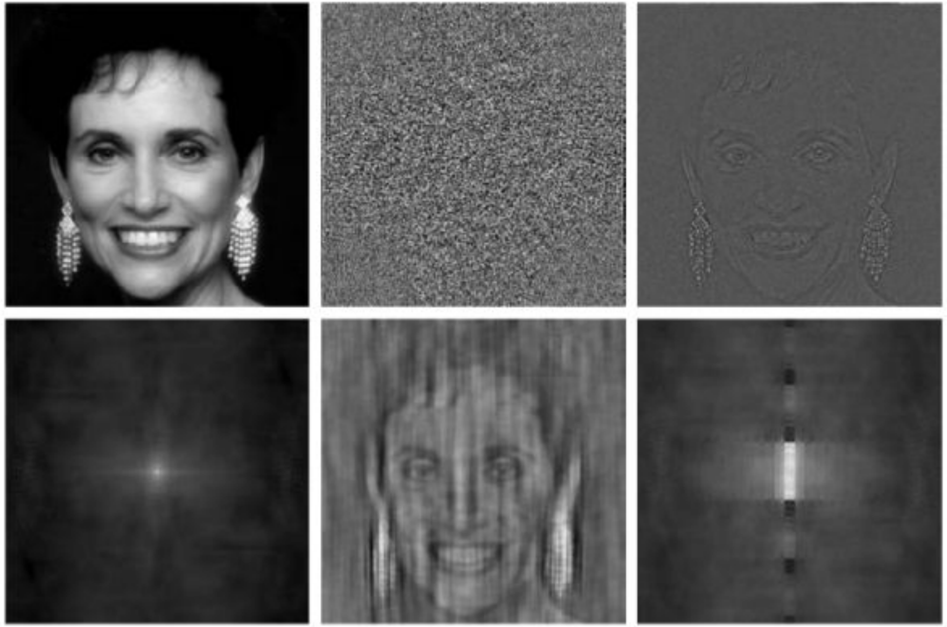

a	b	c
d	e	f

FIGURE 4.27 (a) Woman. (b) Phase angle. (c) Woman reconstructed using only the phase angle. (d) Woman reconstructed using only the spectrum. (e) Reconstruction using the phase angle corresponding to the woman and the spectrum corresponding to the rectangle in Fig. 4.24(a). (f) Reconstruction using the phase of the rectangle and the

Filtros:

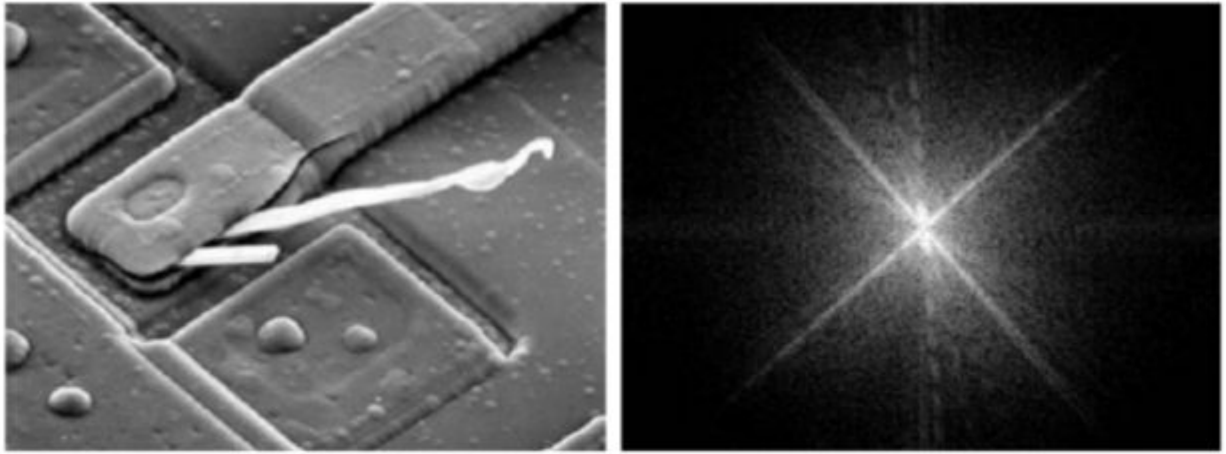

a b

FIGURE 4.29 (a) SEM image of a damaged integrated circuit. (b) Fourier spectrum of (a). (Original image courtesy of Dr. J. M. Hudak, Brockhouse Institute for Materials Research, McMaster University, Hamilton, Ontario, Canada.)

Filtros:

$$G(u, v) = H(u, v) \cdot F(u, v)$$

Resultado filtragem, zerando $F(M/2, N/2)$ – eliminando o nvel DC.

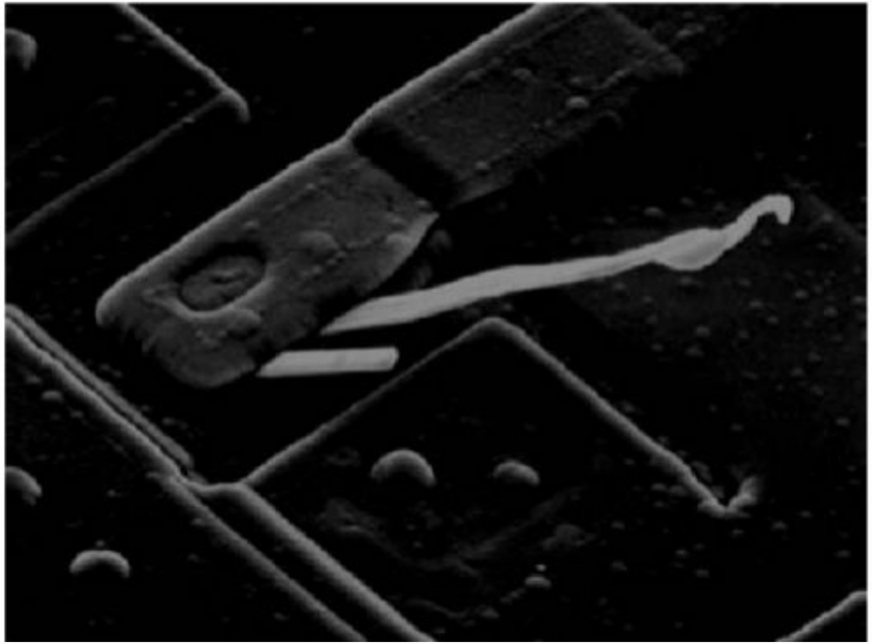

Filtros:

Passa-Baixas Passa-Altas Passa-Altas + DC

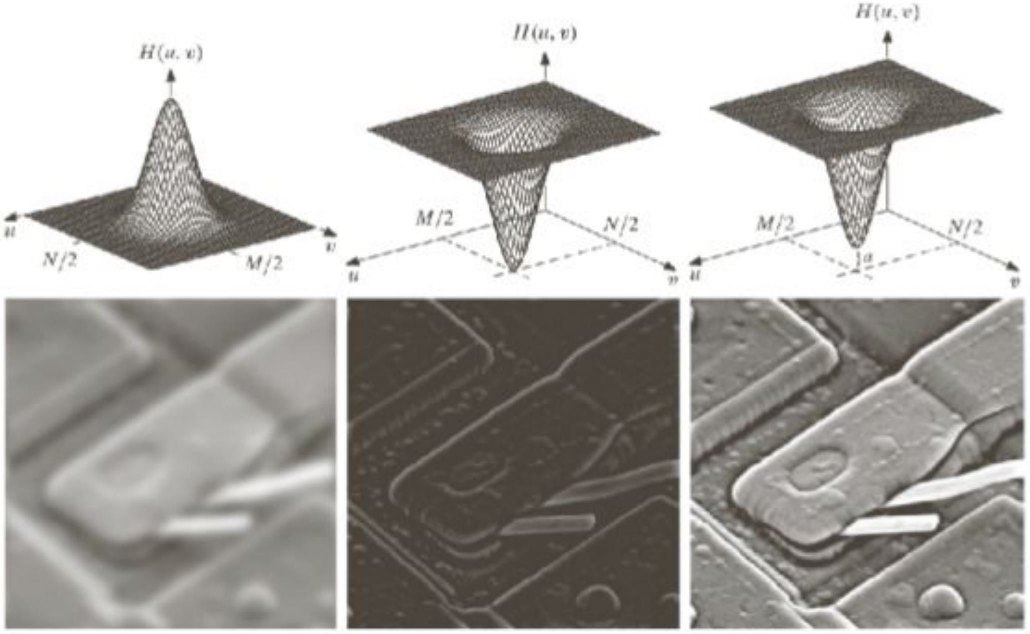

a	b	c
d	e	f

FIGURE 4.31 Top row: frequency domain filters. Bottom row: corresponding filtered images obtained using Eq. (4.7-1). We used $a = 0.85$ in (c) to obtain (f) (the height of the filter itself is 1). Compare (f) with Fig. 4.29(a).

Fase:

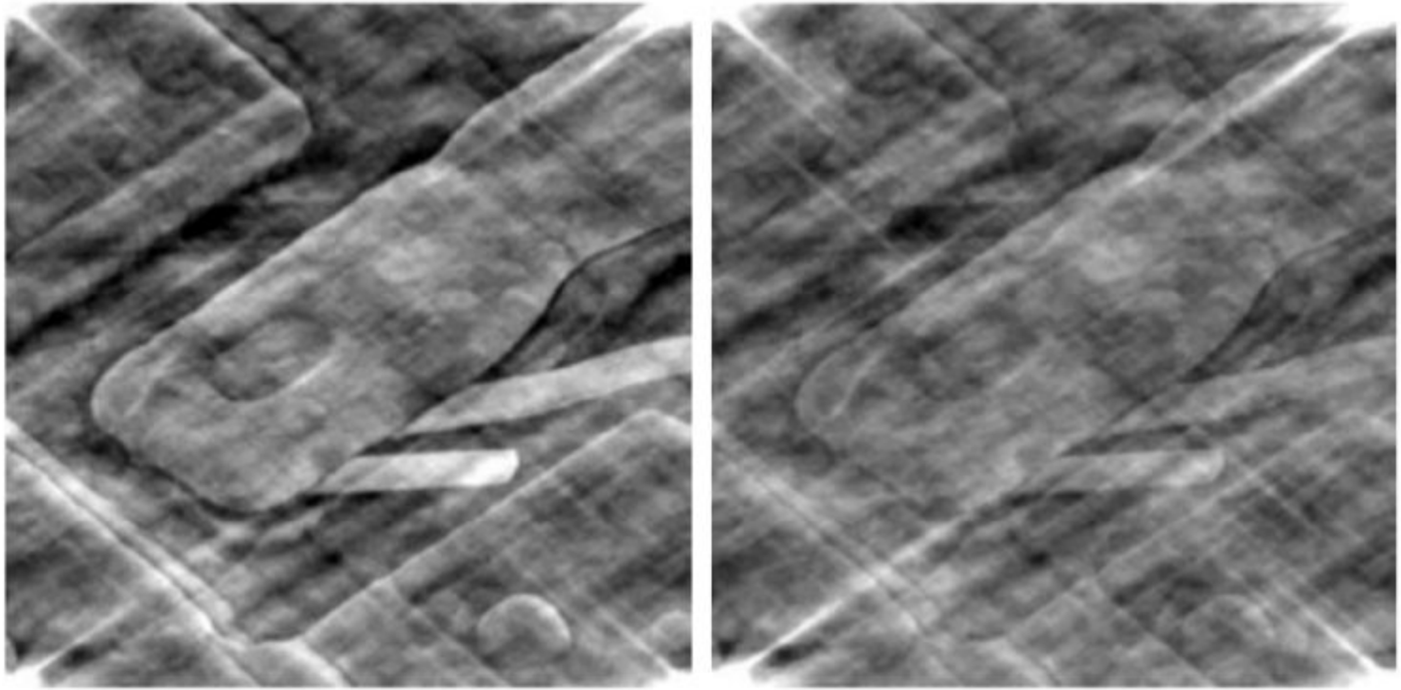

a b

FIGURE 4.35
(a) Image resulting from multiplying by 0.5 the phase angle in Eq. (4.6-15) and then computing the IDFT. (b) The result of multiplying the phase by 0.25. The spectrum was not changed in either of the two cases.

Fase:

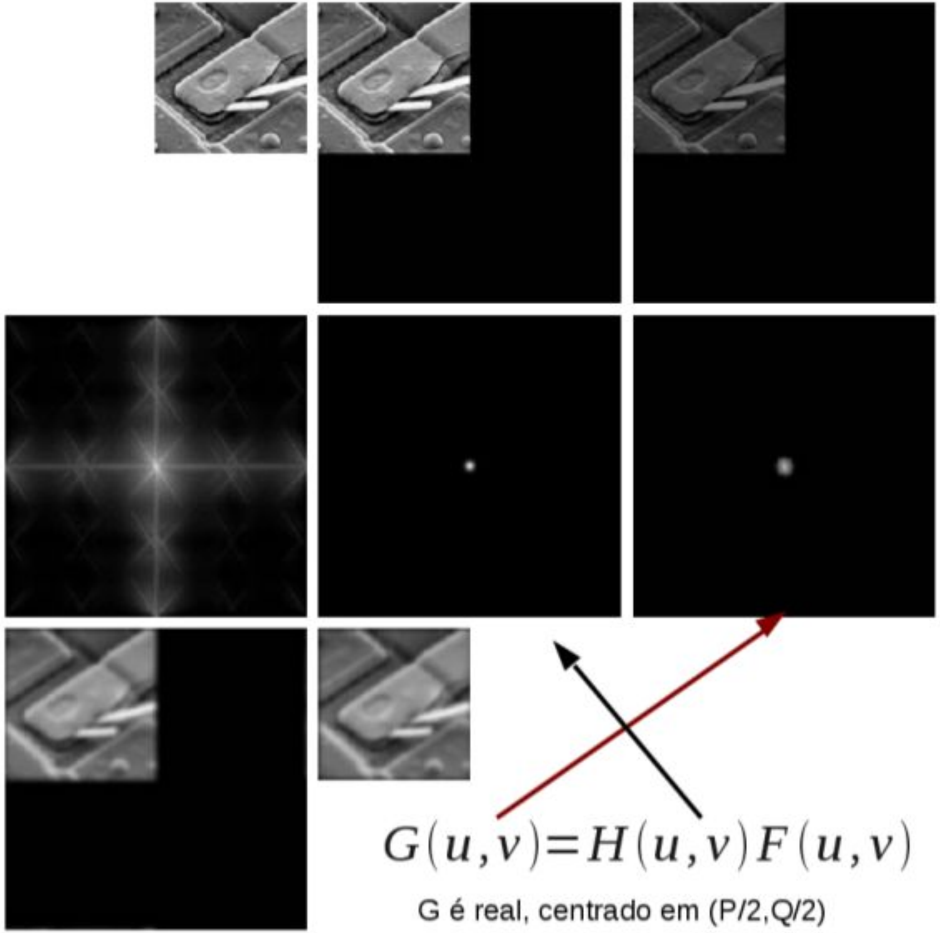

$$G(u,v)=H(u,v)F(u,v)$$

G é real, centrado em (P/2,Q/2)

a b c
d e f
g h

FIGURE 4.36 (a) An $M \times N$ image, f. (b) Padded image, f_p of size $P \times Q$. (c) Result of multiplying f_p by $(-1)^{x+y}$. (d) Spectrum of F_p. (e) Centered Gaussian lowpass filter, H, of size $P \times Q$. (f) Spectrum of the product HF_p. (g) g_p, the product of $(-1)^{x+y}$ and the real part of the IDFT of HF_p. (h) Final result, g, obtained by cropping the first M rows and N columns of g_p.

Filtros:

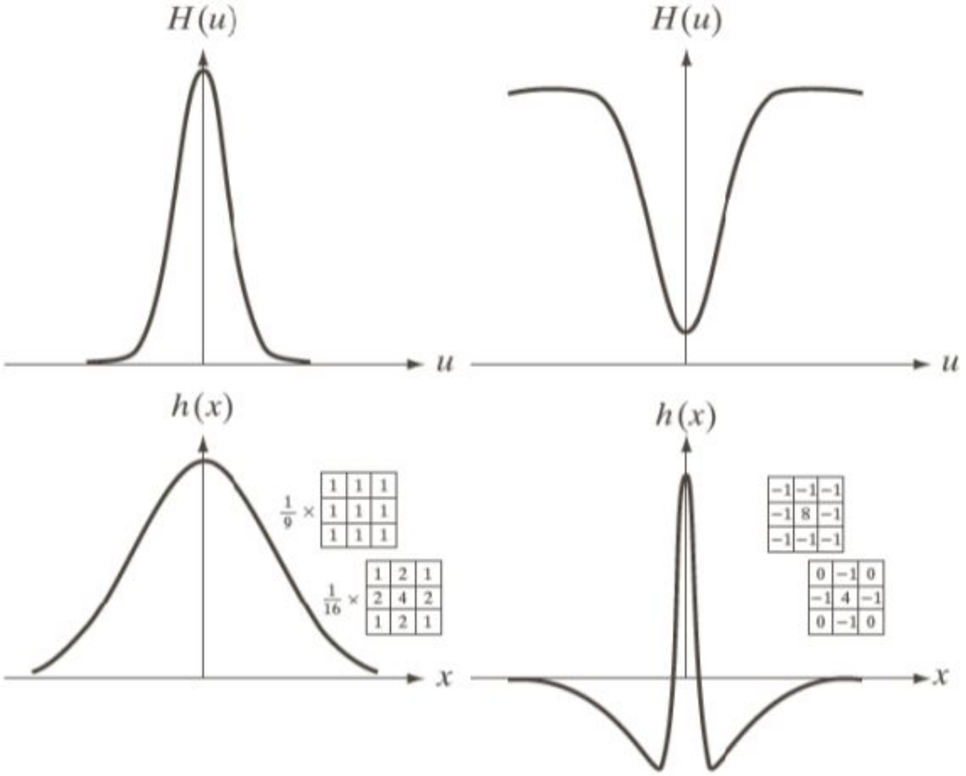

FIGURE 4.37
(a) A 1-D Gaussian lowpass filter in the frequency domain. (b) Spatial lowpass filter corresponding to (a). (c) Gaussian highpass filter in the frequency domain. (d) Spatial highpass filter corresponding to (c). The small 2-D masks shown are spatial filters we used in Chapter 3.

Exemplo:

a b

FIGURE 4.38
(a) Image of a building, and
(b) its spectrum.

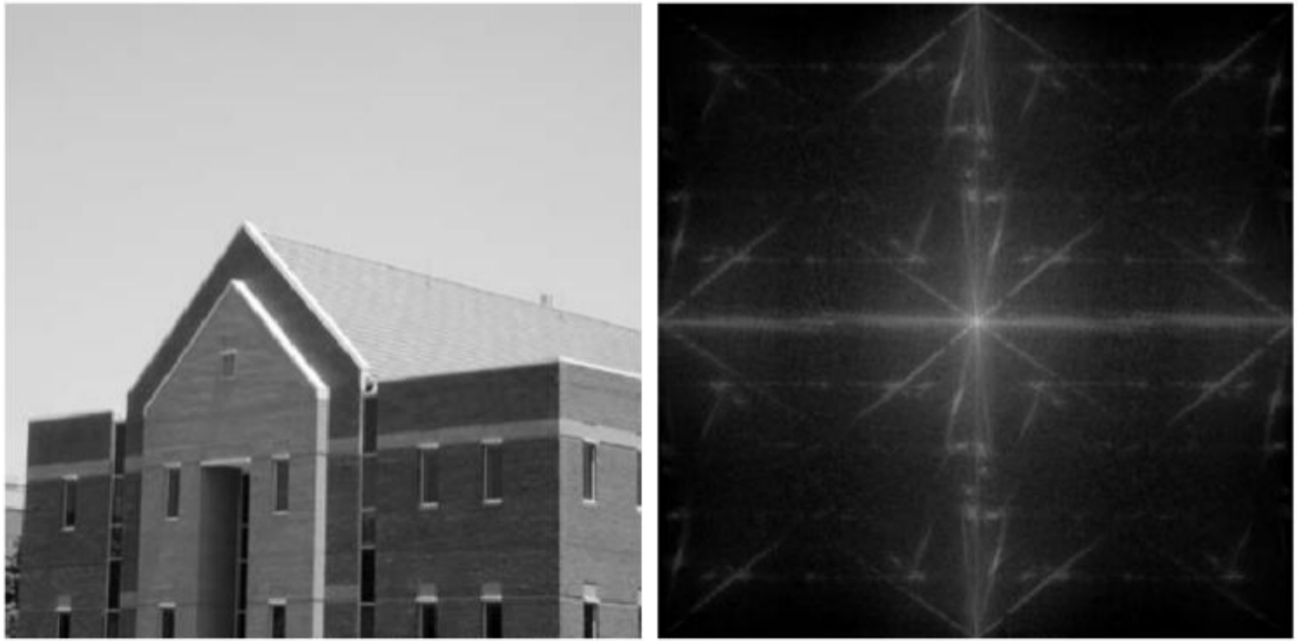

Filtro passa-baixas:

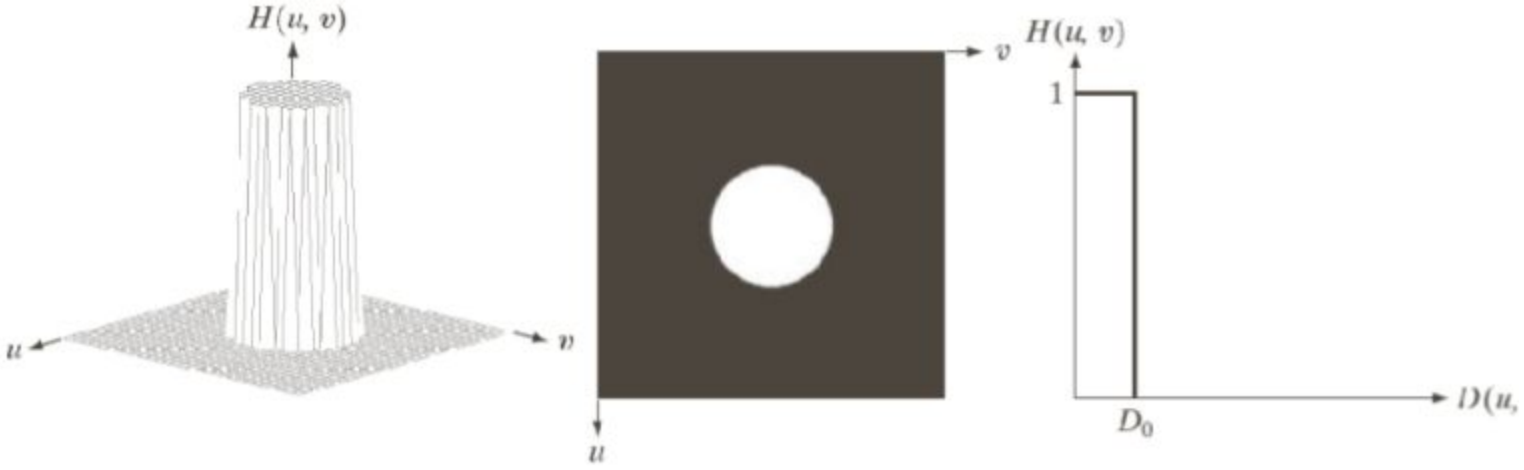

a b c

FIGURE 4.40 (a) Perspective plot of an ideal lowpass-filter transfer function. (b) Filter displayed as an im
(c) Filter radial cross section.

Filtro Ideal:

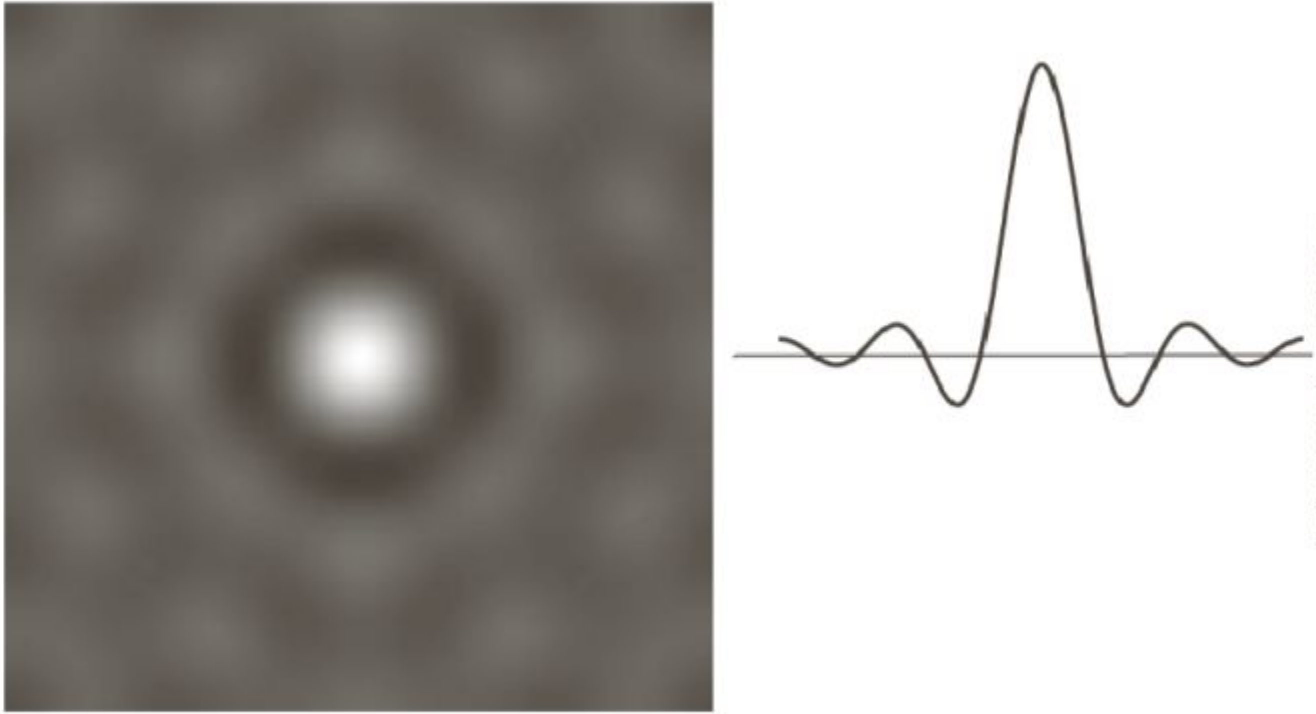

a b

FIGURE 4.43 (a) Representation in the spatial domain of an ILPF of radius 5 and size 1000 × 1000. (b) Intensity profile of a horizontal line passing through the center of the image.

Filtro Ideal:

Filtro Ideal:
Frequências de corte com valores de raio iguais a 10, 30, 60, 160 e 460. A potência removida por estes filtros é 13, 6.9, 4.3, 2.2, e 0.8% do total.

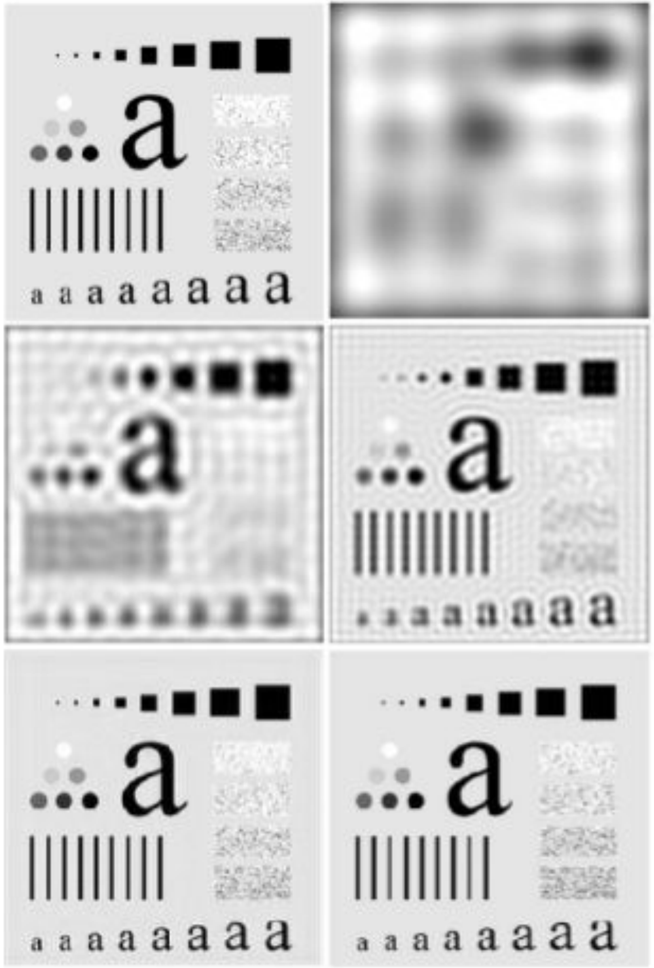

Filtro Butterworth:

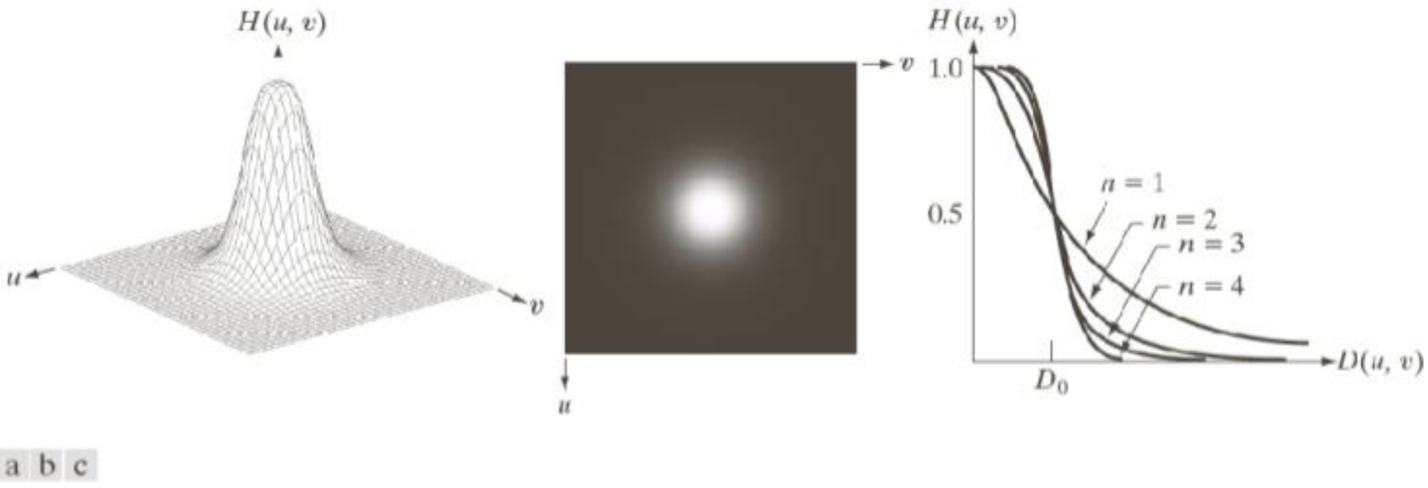

FIGURE 4.44 (a) Perspective plot of a Butterworth lowpass-filter transfer function. (b) Filter displayed as an image. (c) Filter radial cross sections of orders 1 through 4.

$$H(u, v) = \frac{1}{1 + [D(u, v)/D_o]^{2n}}$$

Filtro Butterworth:

Filtro Butterworth:
Frequências de corte com valores de raio iguais a 10, 30, 60, 160 e 460. A potência removida por estes filtros é 13, 6.9, 4.3, 2.2, e 0.8% do total.

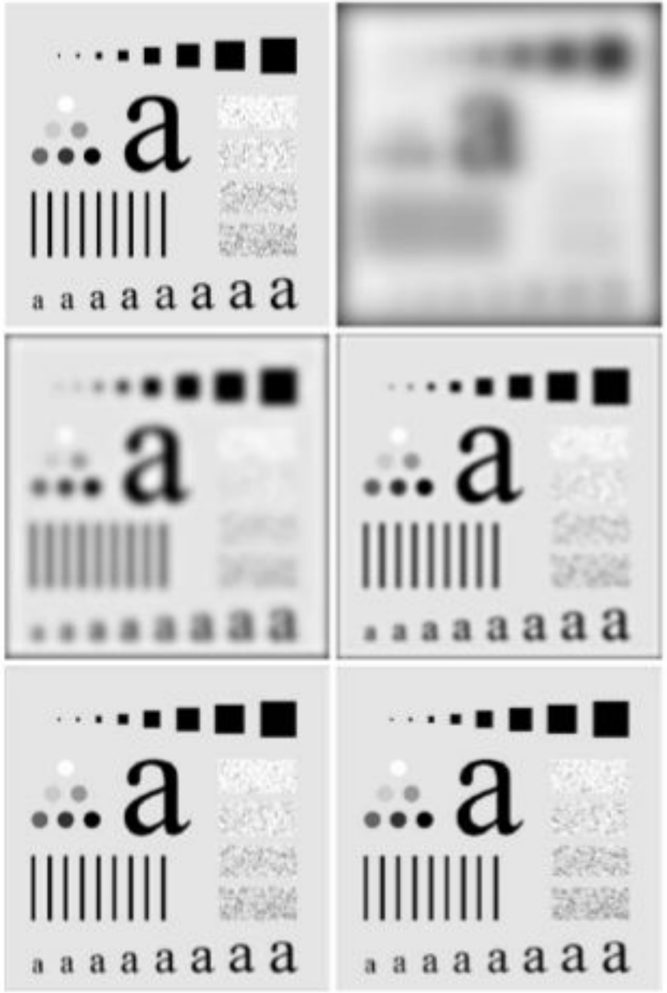

Filtro Gaussiano:

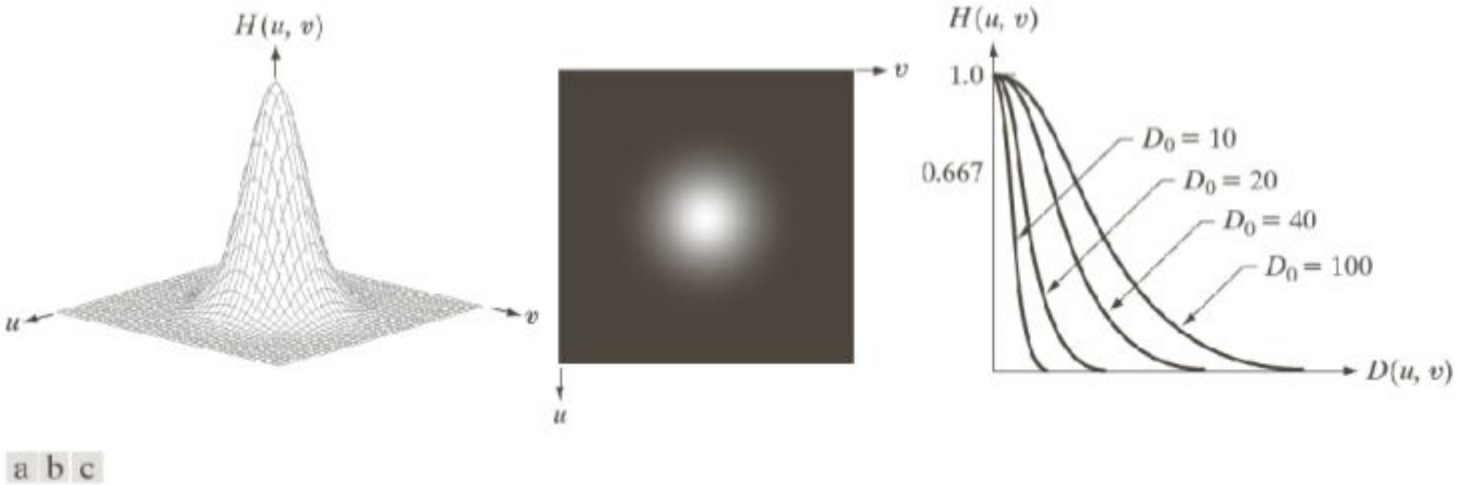

FIGURE 4.47 (a) Perspective plot of a GLPF transfer function. (b) Filter displayed as an image. (c) Filter radial cross sections for various values of D_0.

$$H(u,v) = e^{-D^2(u,v)/2D_o^2}$$

Filtro Gaussiano:

Filtro Gaussiano:
Frequências de corte com valores de raio iguais a 10, 30, 60, 160 e 460. A potência removida por estes filtros é 13, 6.9, 4.3, 2.2, e 0.8% do total.

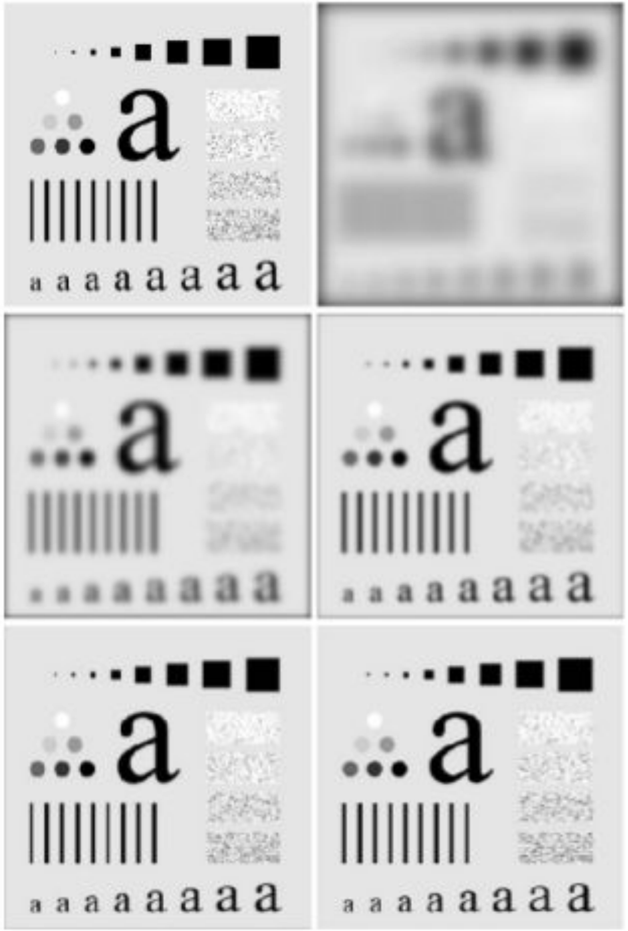

Filtro passa-altas:

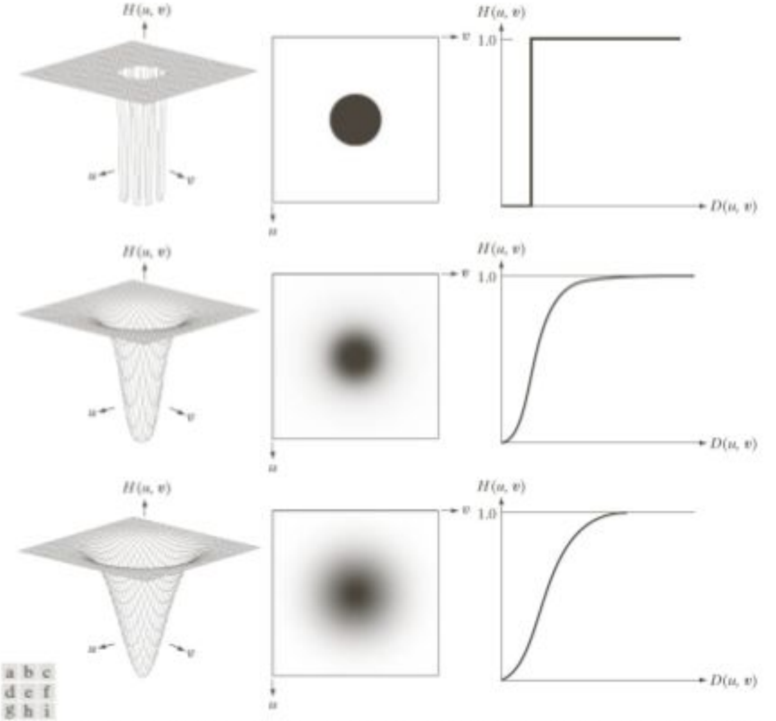

FIGURE 4.52 Top row: Perspective plot, image representation, and cross section of a typical ideal highpass filter. Middle and bottom rows: The same sequence for typical Butterworth and Gaussian highpass filters.

Ideal

Butterworth

Gaussiano

Representação Espacial:

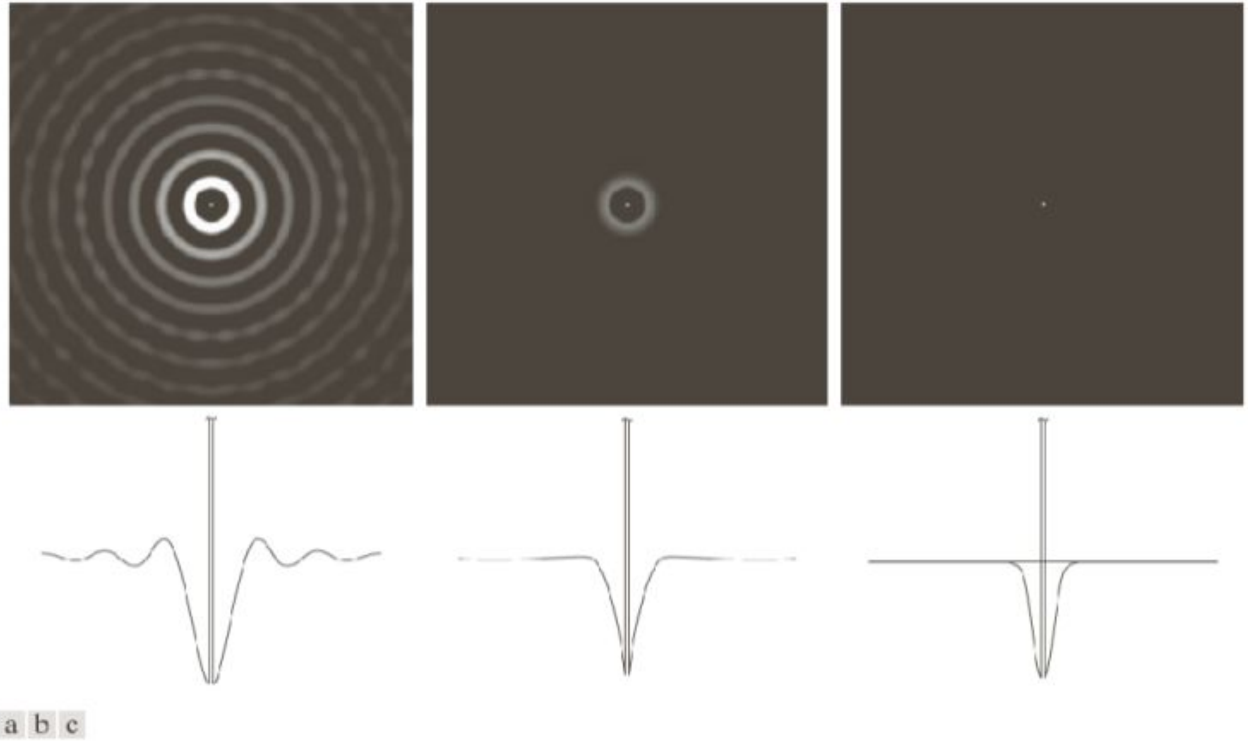

FIGURE 4.53 Spatial representation of typical (a) ideal, (b) Butterworth, and (c) Gaussian frequency domain highpass filters, and corresponding intensity profiles through their centers.

Passa-altas Ideal:

FIGURE 4.54 Results of highpass filtering the image in Fig. 4.41(a) using an IHPF with $D_0 = 30$, 60, and 160.

Passa-altas Butterworth:

a b c

FIGURE 4.55 Results of highpass filtering the image in Fig. 4.41(a) using a BHPF of order 2 with $D_0 = 30, 60$, and 160, corresponding to the circles in Fig. 4.41(b). These results are much smoother than those obtained with an IHPF.

Passa-altas Gaussiano:

a b c

FIGURE 4.56 Results of highpass filtering the image in Fig. 4.41(a) using a GHPF with $D_0 = 30$, 60, and 160, corresponding to the circles in Fig. 4.41(b). Compare with Figs. 4.54 and 4.55.

Fim!

Referências

[1] GONZALEZ, Rafael C.; WOODS, Richard E. Image processing. Digital image processing, v. 2, p. 1, 2007.

[2] Al Bovik, Handbook of Image and Video Processing, Academic Press.